Density functional theory calculations for the hydrogen evolution reaction in an electrochemical double layer on the Pt(111) electrode†

Egill Skúlason,[ab] Gustav S. Karlberg,[a] Jan Rossmeisl,[a] Thomas Bligaard,[ab] Jeff Greeley,[a] Hannes Jónsson*[c] and Jens K. Nørskov*[a]

Received 4th January 2007, Accepted 2nd May 2007
First published as an Advance Article on the web 30th May 2007
DOI: 10.1039/b700099e

We present results of density functional theory calculations on a Pt(111) slab with a bilayer of water, solvated protons in the water layer, and excess electrons in the metal surface. In this way we model the electrochemical double layer at a platinum electrode. By varying the number of protons/electrons in the double layer we investigate the system as a function of the electrode potential. We study the elementary processes involved in the hydrogen evolution reaction, $2(H^+ + e^-) \rightarrow H_2$, and determine the activation energy and predominant reaction mechanism as a function of electrode potential. We confirm by explicit calculations the notion that the variation of the activation barrier with potential can be viewed as a manifestation of the Brønsted–Evans–Polanyi-type relationship between activation energy and reaction energy found throughout surface chemistry.

Introduction

The development of a molecular-level picture of surface electrochemical processes is complicated by difficulties in experimentally probing the processes occurring at the interface between the electrode surface and the electrolyte. Measurements of the rate of electron exchange during a reaction can be done with relative ease, but it is considerably more difficult to obtain information about the state of the surface during reaction. Most of the powerful techniques developed in surface science cannot be used in the presence of a liquid electrolyte, but a few *in situ* methods exist which can probe the state of the interface during electrocatalytic operation.

While considerable progress has been made on the characterization of electrochemical interfaces and processes *in situ*,[1–10] a consensus has not been reached on the predominant reaction mechanism even for the electrochemical formation of hydrogen molecules, the hydrogen evolution reaction (HER), $2(H^+ + e^-) \rightarrow H_2$, on the most common electrode material, Pt. The initial adsorption of a proton to form adsorbed hydrogen, the Volmer reaction, $H^+ + e^- \rightarrow H_{ad}$,[11] is usually considered to be fast[1] but then there are two possibilities for the subsequent, slower hydrogen evolution process: one is the homolytic Tafel reaction, $2H_{ad} \rightarrow H_2$,[12] the other is the heterolytic Heyrovsky reaction, $H_{ad} + H^+ + e^- \rightarrow H_2$.[13] Markovic *et al.* have found from experimental studies of kinetics that HER proceeds *via* the Tafel reaction on the Pt(110) surface but *via* the Heyrovsky reaction on the Pt(100) surface.[14] They could, however, not conclude which mechanism dominates on the Pt(111) electrode. A number of other experimental studies of HER on various Pt single crystal surfaces or polycrystalline Pt films have suggested either the Tafel reaction[2,15,16] or the Heyrovsky reaction.[17] Kunimatsu *et al.* concluded that it is not possible to make definitive statements about the reaction mechanism on the basis of kinetic measurements alone, and recommended that such experiments should be supplemented by the direct observation of the electrode surface at the molecular scale.[2] Some indications have been found for a dual pathway mechanism of the HER or the reverse reaction, the hydrogen oxidation reaction (HOR). Wang *et al.*[18] have constructed kinetic equations taking into account both the Tafel and the Heyrovsky pathways in the HOR on Pt electrodes and the results indicate that the simplest kinetic models may be inadequate in describing the reaction.

It is generally found that the reaction order in electron transfer, the transfer coefficient, is between 0 and 1 for all electrochemical reactions, and typically close to 0.5.[19,20] The apparent activation energy for the HER on Pt(111) at the equilibrium potential has been determined to be ~0.2 eV under acidic conditions.[14] Two different adsorbed hydrogen species on Pt(111) have been invoked; the underpotential deposited hydrogen H_{upd} [21] and the overpotential deposited hydrogen H_{opd}.[22,23] During a potential sweep in the negative direction the H_{upd} state is observed starting at *ca.* +0.35 V relative to the equilibrium potential for the reaction at room temperature.[1,14] The H_{opd} refers to adsorbed hydrogen at and below the potential where hydrogen evolution becomes thermodynamically possible, and it has been suggested to be more reactive than the H_{upd}.[1,2]

[a] *Center for Atomic-scale Materials Design, Department of Physics, Building 307, NanoDTU, Technical University of Denmark, DK-2800 Lyngby, Denmark. E-mail: norskov@fysik.dtu.dk*
[b] *Science Institute, University of Iceland, Dunhaga 3, IS-107 Reykjavik, Iceland*
[c] *Faculty of Science, VR-II, University of Iceland, IS-107 Reykjavik, Iceland. E-mail: hj@hi.is*

† Electronic supplementary information (ESI) available: The variation of the activation energy and reaction energy with number of Pt layers used for the DFT calculations (Fig. S1) and the variation of the work function with increasing vacuum distance between the repeated slabs (Fig. S2). See DOI: 10.1039/b700099e

Electronic structure calculations offer the possibility of providing a detailed molecular-level description of the processes involved. This, however, requires large-scale calculations of realistic systems including the electrolyte with sufficient accuracy to give results that are at least qualitatively correct. In addition, it requires a systematic study of the effect of the electrode potential in these processes. Several important steps have been taken in this direction. Cai and Anderson have performed quantum chemical calculations to study elementary processes relating to HER on small Pt clusters finding *e.g.* an activation energy for the Heyrovsky reaction at the equilibrium potential in agreement with the value determined experimentally for the Pt(100) surface.[24] The model used to describe the Pt surface in these studies is extremely small, just a single Pt atom. Several groups have, on the other hand, described the electrode by density functional theory (DFT) calculations of an extended slab[25] with the possibility of contact with a bilayer or more of water molecules.[26–32] Recently, a method for extracting thermo-chemical data as a function of the applied potential has been introduced from such calculations.[26,33] Filhol and Neurock have taken the further step of including the possibility of charging the slab while smearing a countercharge homogeneously over space as a method of introducing an electrical potential in the system.[28] Otani and Sugino have taken another approach where an external potential is included in the super cell, dragging the electrons from one side of the slab to the other, creating a charged surface.[34]

In the present paper we introduce a set of DFT calculations where the charge and potential of the surface is varied by adding hydrogen atoms to a water bilayer outside a metal slab. Since the hydrogen atoms get solvated to form protons and the electrons move to the surface we create in this way a double layer and by varying the proton/electron concentration we can study the system as a function of surface charge and hence electrode potential. We use the method to elucidate the reaction mechanism of the HER on Pt(111) by presenting results for the reaction path and activation energy of the various elementary reactions. We study the Volmer reaction and the coverage and potential dependence of the hydrogen adsorption energy, elucidating the nature of the different adsorbed states. For the subsequent hydrogen formation step, both the Heyrovsky and the Tafel reactions show a linear variation in the activation barrier with the applied potential. The results indicate that the two mechanisms have similar activation barriers, with the one for the Heyrovsky reaction being slightly lower at the equilibrium potential. Finally, we show that a linear variation of the activation energy with potential can be viewed as a manifestation of a linear Brønsted–Evans–Polanyi-type relationship between the activation energy and the reaction energy.

Model and calculational details

We base our studies on DFT calculations in a plane wave pseudopotential implementation,[35,36] employing ultrasoft pseudopotentials[37] to represent the ionic cores. All calculations were performed with the RPBE exchange–correlation functional.[38,39] The self-consistent electron density is determined by iterative diagonalization of the Kohn–Sham Hamiltonian, with the occupation of the Kohn–Sham states being smeared according to a Fermi–Dirac distribution with a smearing parameter of $k_BT = 0.1$ eV, and Pulay mixing of the resulting electronic density. All total energies have been extrapolated to $k_BT = 0$ eV.

In all cases an irreducible Monkhorst Pack k-point grid was used to reduce the number of k-points in the calculations. The calculations were carried out in periodically repeated surface (3×2), (6×2), (3×4) and (6×4) super cells with 4×6, 2×6, 4×3 and 2×3 k-point sampling, respectively. Calculations for hydrogen adsorption and desorption in the absence of a water overlayer were performed using a (2×2) surface super cell and a 4×4 k-point sampling. The Pt(111) electrode was represented by a slab consisting of three atomic layers in all cases. The addition of 5 more Pt layers was found to change the adsorption energy and energy barrier in a few test cases by less than 0.1 eV (see Fig. S1 in the ESI†). The two bottom layers of the Pt slab were fixed but the top layer was allowed to relax. The dipole correction was used in all cases to decouple the electrostatic interaction between the periodically repeated slabs. The RPBE lattice constant of Pt of 4.02 Å was used and the slabs were separated by 10–12 Å of vacuum, depending on the system (see Fig. S2 in the ESI†). The plane wave cutoff was 26 Ry (354 eV) both for the wave function and for the density. An increase to 30 Ry for the wave function cutoff and 60 Ry for the density cutoff changed values of the reaction energy by less than 0.01 eV.

In order to model the water–solid interface as a function of electrode potential, we set up the following simple model. The Pt-electrode/electrolyte interface is modeled using a Pt(111) slab with a bilayer of water and excess H atoms included in the water layer as shown in Fig. 1. This results in the formation of solvated protons in the water layer and transfer of electrons to the metal. By varying the number of hydrogen atoms added, the electrostatic potential of the double layer can be varied. The potential at which the calculations are made is deduced from the work function, or in some cases, hydrogen coverage of the model system.

The approach outlined above results in the formation of solvated protons as can be directly observed by the formation of an electrostatic dipole layer outside the surface. The variation of the electrostatic potential profile as a function of distance perpendicular to the surface is shown in Fig. 2 for two different charge states and hence two different potentials. We note that the system used in our simulations is overall charge neutral. For a Pt(111) electrode in an acid solution at electrode potentials below the potential of zero charge (pzc), our model quite realistically describes the (Helmholtz) double layer set up by the electrons in the electrode surface and the same number of solvated protons just outside the surface. This model is realistic, and a similar system has been studied experimentally.[40] The neutral double layer is found generally in electrochemical cells; it is a consequence of the fact that in the conducting electrolyte there cannot be a long range electrical field, hence the surface charge is screened by the counter ions. The main approximation in our model is that the protons are only allowed to be solvated in the first water bilayer at the electrode surface. The use of only a single water

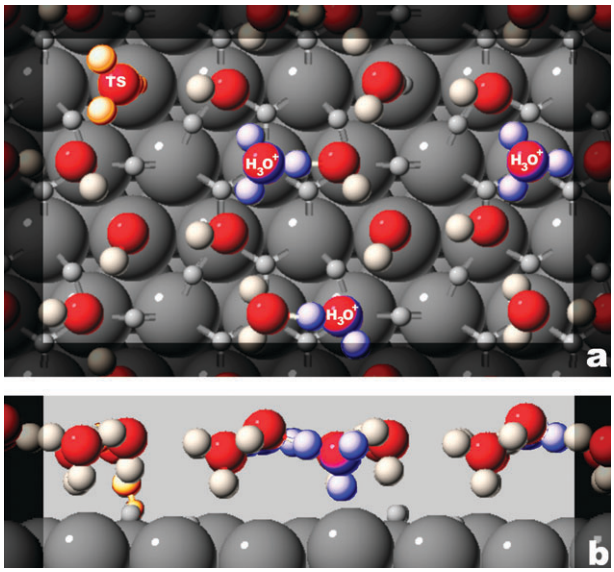

Fig. 1 Top (a) and side (b) view of the model system for the electrochemical double layer above a Pt(111) electrode. This example contains 3 hydronium ions (marked H_3O^+) in a water-bilayer over a hydrogen covered 3 layer Pt(111) slabs in a 6 × 4 supercell. The TS marking shows the transition state for the Heyrovsky reaction. The hydrogen coverage is 7/6 ML, with 1 ML of hydrogen atoms in face centred cubic (FCC) or bridge sites plus 1/6 of a ML in on-top sites. All adsorbed H atoms are shown as light grey and have been made smaller to distinguish them from the H atoms in the water bilayer. Some hydrogen atoms are pushed from FCC holes to bridge sites because of the interaction with the H in the on-top position.

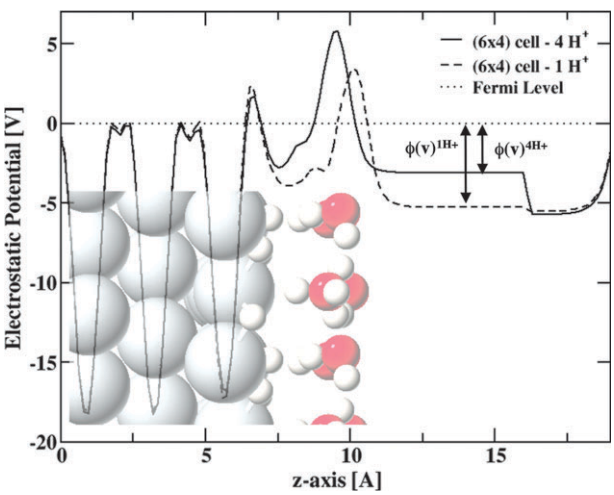

Fig. 2 The variation of the electrostatic potential profile averaged parallel to the surface as a function of the *z*-axis of the super cell. Starting from the left we have the Pt slab, adsorbed hydrogen atoms, the protonated water layer, and the vacuum region separating one slab from the next. The electrostatic potential is shown for two different charge states and hence two different electrode potentials. The $\phi(v)^{1H+}$ and $\phi(v)^{4H+}$ represent the absolute value of the electrostatic potential in the vacuum region relative to the Fermi level for systems with 1 and 4 protons solvated in the water bilayer, respectively. In the vacuum region a dipole layer is introduced in the calculation in order to electrostatically decouple the periodically repeated slabs in the *z*-direction.

bilayer is a simplification dictated by the high computational cost of the DFT calculations and the resulting limitations on the system size. We note that because of the neutrality requirement, the concentration of protons in the double layer is given by the potential (or the surface charge) of the electrode and is different (higher below the pzc) than in the bulk solution.

Compared to recent models introduced to do DFT calculations of charged electrode surfaces, the present model has the advantage that it explicitly describes the surface and counter ions and the electrical field created by them. In the method of Filhol and Neurock[28] charge is added to the metal surface and (implicitly) the counter charge is smeared out over all space as a homogeneous background. In the method of Otani and Sugino[34] an external dipole layer is introduced to create a charged surface, and the counter charge is therefore located approximately 10 Å away from the electrode. Both methods provide a large step forward towards a microscopic description of the electrochemical cell, but in the first case the double layer is smeared out considerably by the fact that the counter charge is not localized, and in the second case the Helmholtz layer becomes very broad.

To be able to attain different values of the electrode potential we vary the proton concentration in the double layer. In order to describe a reasonable range of potentials, the unit cell of the slab has to be large. We have added 1, 2, 3, and 4 protons and electrons in a large super cell (6 × 4), 1 and 2 protons and electrons in intermediate sized super cells (6 × 2 or 3 × 4), and 1 proton and electron in a small super cell (3 × 2).

The electrode potential (U) of the slab relative to the normal hydrogen electrode (NHE) can be estimated from the work function, ϕ, relative to that of the NHE

$$U = \phi - \phi_{\mathrm{NHE}} \qquad (1)$$

This procedure was outlined by Trasatti[41] and has been used previously by *e.g.* Filhol and Neurock[28] and Cai and Anderson.[24] We use a value of $\phi_{\mathrm{NHE}} = 4.5$ V as the work function of the reference system (NHE *vs.* vacuum), chosen to be within the range 4.44–4.85 V found in the literature.[42,43] The fact that we can only treat a small system with few protons per unit cell has implications for the calculated work function. It means that when studying proton/electron transfer reactions, the potential changes during the reaction. This is particularly problematic for the smallest unit cell, and we therefore primarily use the large unit cells where only one of the protons reacts, in order to establish the potential dependence of the activation energies in the following. We, furthermore, take the average of the initial and final state potentials as representative of the potential at which the reaction occurs. In this context we also note that the work function could depend on the number of water layers included. Hence, the uncertainty in U stems not only from ϕ_{NHE} but also from the absolute value obtained from the calculations. A final interesting issue to consider regarding the extraction of the potential from the work function is the coverage of H on the surface since it also affects the work function. Indeed, as will be shown in the following, one can actually relate the hydrogen coverage to the potential *versus* the standard hydrogen electrode. Hence, in

order to read off the correct potential from the work function for a certain proton concentration, a H coverage consistent with the chemical potential of H in solution (assuming this step to be in equilibrium) is needed on the surface. The method described above allows us to vary the potential relative to the NHE in the range from −2.3 V (two protons in an intermediate size unit cell, high H coverage or 22/12 ML) to +0.5 V (one proton in an intermediate size unit cell, low H coverage or 1/12 ML).

In the present study we investigate the Volmer, Tafel, and Heyrovsky reactions under varying potentials using the model described above. The calculations include a complete nudged elastic band (NEB) calculation[44,45] of the reaction paths and the reaction barriers. Due to computational limitations set by the DFT calculations we have made the following simplifications: A starting guess of the initial, final, and transition states of the relevant reaction paths is found using the smallest super cell (3 × 2). These calculations include complete relaxation of the first metal layer, the adsorbed hydrogen, and the water bilayer during the reaction. We use the relaxed structures of the initial, transition and final states from the (3 × 2) cell calculations as a starting guess for the larger cell calculations where we can vary the composition and hence the charge and potential of the electrode. The initial and the final states are completely relaxed, while the transition states (TS) are calculated in a more approximate way. The main core of the TS in the Heyrovsky reaction, the Pt–H–H–OH_2 configuration obtained by NEB calculations for the small cell (see the TS marking in Fig. 1), is fixed in these larger cells while the surrounding water, hydronium ions, adsorbed hydrogen and the first Pt layer are allowed to relax. After relaxation, the residual forces on the fixed TS atoms are less than 1 eV $Å^{-1}$ in all cases. Since the TS corresponds to a saddle point of the potential energy surface, we expect this to give rise to quite small errors in the TS energy, but this procedure leaves room for improvement.

The Volmer reaction

First, we consider the Volmer reaction:

$$H^+ + e^- \rightarrow H_{ad}$$

We have studied this reaction at different hydrogen coverages and for different numbers of protons and electrons (different potentials). Fig. 3 shows examples of transferring solvated protons to the Pt(111) electrode at negative potentials with initial hydrogen coverages of 5/6 ML and 1 ML. The activation barriers are quite low, below 0.15 eV for both systems. The main contribution to these activation barriers come from an initial proton transfer from one water molecule to another before a proton can be transferred to the electrode. This can be seen in the inserts of Fig. 3. The actual transfer of the proton to the surface, from the TS to the final state (FS), is downhill in energy. We invoke the initial proton transfer to another water molecule in the water bilayer in order to end up in the energy optimized final state of the ice-like structure of the water bilayer where every other water molecule in the hexagonal framework points down and the others are parallel to the surface. The barrier of about 0.15 eV including rearrangements in the water layers is consistent with calculated barriers for proton transfer in water.[46–48]

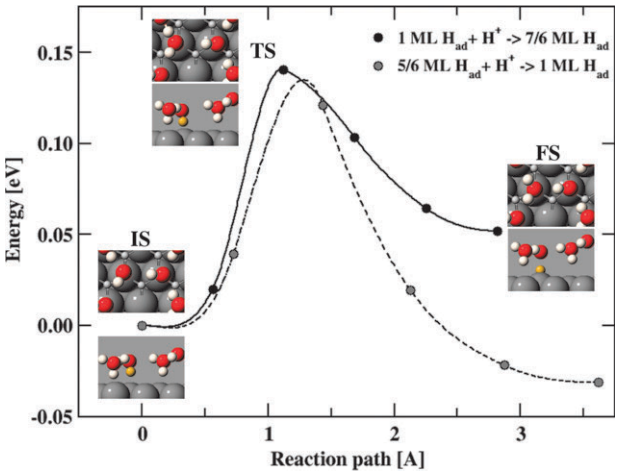

Fig. 3 Reaction paths from NEB calculations for the Volmer reaction, $H^+ + e^- \rightarrow H_{ad}$, at two different hydrogen coverages. The initial states contain solvated protons and 1 ML (solid curve) or 5/6 ML (dashed curve) of hydrogen atoms cover the surface in the FCC holes. In the final states the solvated protons have adsorbed into on-top sites. The average potential is −0.2 V *vs.* NHE (solid curve) and +0.2 V *vs.* NHE (dashed curve). Inserts show top and side views of the initial (IS), transition (TS), and final state (FS) structures for the 1 ML coverage system. The average distance from the first Pt layer to the O atoms in the water bilayer is 3.59 Å for the IS and 3.99 Å for the FS. For the system with 5/6 ML coverage, the proton is transferred to an on-top site with an empty FCC hole next to it. It will subsequently move to the FCC site and gain ∼0.1 eV in potential energy.

Our calculations for the Volmer reaction suggest that the energetics is given essentially by the reaction energy with a small extra contribution to the energy barrier due to the proton transfer in the water bilayer. This means that close to the equilibrium potential, the barrier for this process is small, a finding that is in good agreement with conclusions from experiments.[1] We therefore expect this reaction to be in equilibrium even at room temperature. This means that the coverage of hydrogen on the surface is given by the chemical potential of hydrogen, which at standard conditions (298 K, pH = 0) is determined by the potential, U, relative to the normal hydrogen electrode:

$$\mu_H = -eU \qquad (2)$$

This expression is analogous to the Nernst equation for pH = 0.

We have calculated the differential hydrogen adsorption energy and free energy (using the method outlined in ref. 26) as a function of coverage in the absence of water and potential as shown in Fig. 4. We have found that water and an additional electrostatic field have only small effects on the hydrogen adsorption energy,[49] so this is a good representation of the adsorption free energy at the electrode surface.

Eqn (2) gives us a direct link between the electrode potential and the hydrogen coverage since states with a free energy $\Delta G_H < \mu_H = -eU$ will tend to be filled. According to Fig. 4, at 0.25 ML hydrogen coverage the potential U is approximately

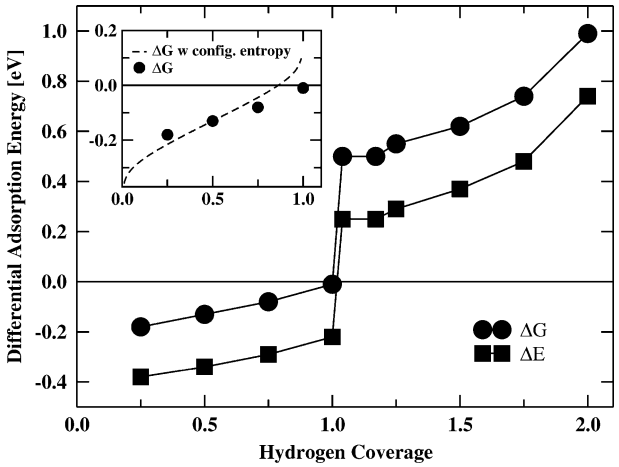

Fig. 4 Calculated differential adsorption energy of hydrogen as a function of coverage over a Pt(111) surface in vacuum. Both the energy and the free energy (at 300 K) are shown relative to 1/2 H_2 in the gas phase (at standard conditions). In the inset the contribution from the configurational entropy has been included in the free energy (dashed).

+0.18 V and an increase to a coverage of 1 is achieved close to $U = 0$ V.

This is in quite good agreement with the work of Markovic *et al.*[14] whose cyclic voltammetry (CV) measurements indicate 0.25 ML coverage of H_{upd} on Pt(111) at approx. 0.20–0.25 V. Experiments have also indicated that the H coverage at $U = 0$ V is ~0.66 ML.[1] In fact, if the contribution from the configurational part of the entropy term is included in ΔG an even better agreement is achieved. To model the configurational part of the entropy we use

$$S_{conf.} = -k_B(\theta \ln(\theta) + (1-\theta)\ln(1-\theta))$$

Since we are looking at the differential free energy, we need $dS_{conf.}/d\theta$, which is given by:

$$dS_{conf.}/d\theta = k_B \ln((1-\theta)/\theta)$$

In the inset of Fig. 4 this part is added to ΔG. Now the calculated H coverage at $U = 0$ V is ~0.8 ML.

From the adsorption energies shown in Fig. 4 a value of the pair-wise nearest neighbor interaction between adsorbed H atoms in the FCC sites can be extracted. We find the H–H interaction to be very weak, about 0.02 eV. This is very close to values (0.04 eV) extracted from CV.[50]

At hydrogen coverage above 1, the H atoms are found to be most stable in an on-top adsorption site, but the calculations suggest that this high coverage state is not occupied except at potentials below ~−0.5 V. The reason is that at a hydrogen coverage of 1, we find a discontinuity in the adsorption energy of close to 0.5 eV. This we associate with a strong, repulsive H–H interaction when the H–H distance becomes small.

As mentioned in the Introduction, the terms H_{upd} and H_{opd} are frequently used when discussion the HER and the HOR.[15] Since H_{opd} is the adsorbed hydrogen species below the equilibrium potential, it must be associated with the active species in the HER reaction. The question is whether it is fundamentally different from H_{upd}. The calculations indicate that apart from a weak H–H repulsion, nothing special happens to the adsorbed state of hydrogen on Pt(111) up to a coverage of 1.

In situ infrared reflection-absorption spectroscopy (IRAS) experiments[51] have found two different adsorbed states, one assigned to H_{upd} (around 1000–1300 cm^{-1})[52–54] and another one assigned to H_{opd} with a considerably higher vibrational frequency (around 2100 cm^{-1}).[2] The assignment of H_{opd} was supported by the finding that the intensity of the high frequency band increased linearly with decreasing potential.

In order to look more into this we have calculated the perpendicular vibrational frequency for adsorbed hydrogen in on-top and FCC sites. We find these frequencies to be 2200 and 1017 cm^{-1}, respectively, in good agreement with the experiments. But, as noted above, our calculations suggest that the on-top H is not the equilibrium site at potentials just below 0 V. One possible explanation of the IRAS observations is therefore the following: DFT calculations show the difference in adsorption energy (including zero point energy) for hydrogen adsorbed in the on-top and FCC sites to be very small, about 0.1 eV.[55] Thus, with a certain coverage of H adsorbed in the FCC sites, the coverage of H in the on-top site is given by $\theta_{top} = \theta_{FCC}\exp(-\Delta G/k_B T)$, where $\Delta G \sim 0.1$ eV, if equilibrium is assumed. At room temperature the on-top occupancy is therefore about 1% of the FCC occupancy. To understand why only the on-top hydrogen is observed when it is only a minority species, we have calculated the dynamical dipole matrix element M for the perpendicular vibrations. We find M to be 0.004 e and 0.032 e for the FCC and on-top adsorption sites, respectively. Since the IR absorption is proportional to the square of the dynamical dipole matrix element, this means that the intensity of the vibration in the on-top site is nearly two orders of magnitude stronger than in the FCC site. Hence, in this picture the on-top H, and hence the $H_{opd,}$ is a thermally populated minority species. The linear relation observed between the intensity of the high frequency band and the potential is in this picture associated with a linear relation between the occupation of on-top sites and the occupation of FCC sites, which in turn is linear in the potential as can be deduced from Fig. 4 for hydrogen coverage between 0.25 and 1 ML.

The Tafel reaction

Next we consider the Tafel reaction:

$$2H_{ad} \rightarrow H_2$$

In the small unit cell at high coverage of hydrogen, the energy barrier is found to be 0.55 eV, considerably higher than for the Volmer reaction, see Fig. 5. Since there is no electron transfer involved, we do not expect the activation barrier for the process to show much potential dependence as long as the hydrogen coverage is constant. Using the intermediate sized unit cells we have calculated the activation energy of the Tafel reaction to be 0.52, 0.60, and 0.68 eV at initial state electrode potentials (deduced from the work function) of +1.8, −0.1 and −1.3 V *vs.* NHE, respectively, with the same initial hydrogen coverage (13/12 ML). Since the electrode potential window is very wide, the calculated changes in the activation

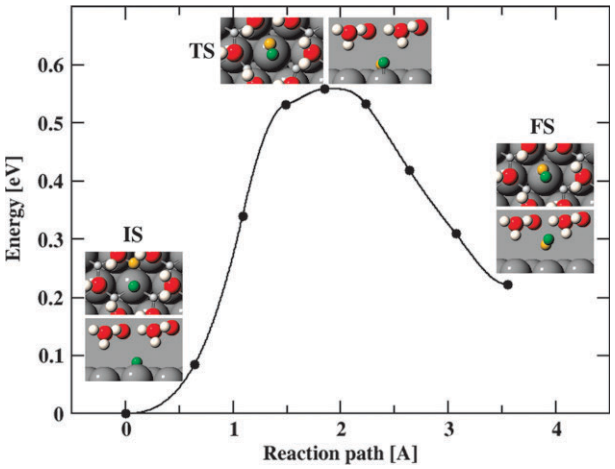

Fig. 5 Reaction path from an NEB calculation showing the energy barriers for the Tafel reaction, $2H_{ad} \rightarrow H_2$. The hydrogen coverage is initially 7/6 of a ML. An on-top hydrogen atom and hydrogen atom in an FCC site react and form a H_2 molecule that desorbs from the surface. The average distance from the first Pt layer to the O atoms in the water bilayer is 4.52 Å for the IS and 4.59 Å for the FS.

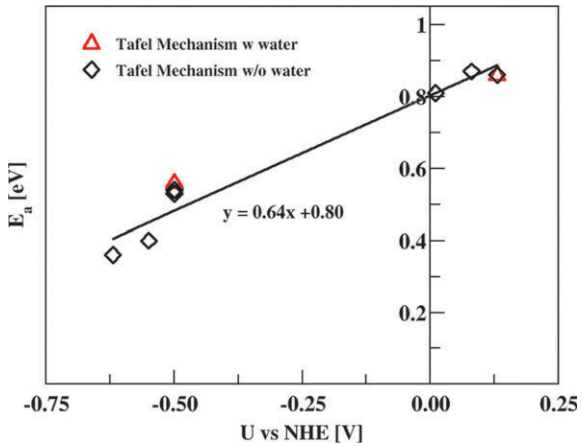

Fig. 7 Activation energy for the Tafel reaction as a function of potential with (triangles) and without (diamonds) a water bilayer. The graph is obtained by combining the hydrogen coverage dependence of the activation (shown in Fig. 6) with the potential scale obtained from the coverage dependence of the differential free energy for hydrogen adsorption (shown in Fig. 4; the configurational entropy has been neglected here) and its relation to the electrode potential (described in the text).

energy are rather small and are perhaps within the error of our calculations.

The Tafel process is equivalent to the traditional Langmuir–Hinshelwood mechanism for H_2 desorption from a Pt(111) surface into a vacuum, and we find that the barrier is not changed significantly by the presence of the water. In Fig. 6 we show the calculated value of the barrier for H_2 desorption as a function of the hydrogen coverage both with and without the water bilayer. Experimentally, the barrier for desorption into vacuum has been measured to be 0.45–0.80 eV.[56,57]

Even though there is only a small direct dependence of the barrier for hydrogen desorption on the applied potential, there is an indirect dependence through the connection between the hydrogen coverage and the potential described above. We can construct the dependence of the barrier for H_2 desorption on the potential under the assumption discussed above that the Volmer reaction is in equilibrium. From Fig. 4 we can get the H coverage as a function of electrode potential, and from the variation of the activation barrier with hydrogen coverage in Fig. 6 we can get the desired relationship. The result is shown in Fig. 7.

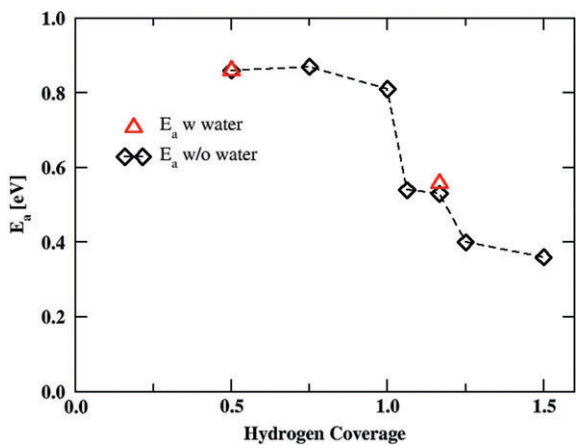

Fig. 6 Calculated activation barrier for the Tafel reaction for H_2 desorption from a Pt(111) surface into a vacuum (diamonds) and in the presence of a water bilayer (triangles, for 3/6 and 7/6 ML) as a function of initial hydrogen coverage.

The variation of the activation barrier for hydrogen desorption is consistent with a linear dependence on the electrode potential. The gap between the two groups of data points in Fig. 7 is due to the discontinuity in the hydrogen coverage at 1 ML and at $\theta_H > 1$ ML (see Fig. 4). From the slope, one can derive a value for the transfer coefficient, α, for the reaction, which we define here as the derivative of the activation energy, E_a, with respect to the potential, U:

$$\alpha = \mathrm{d}E_a/\mathrm{d}(eU)$$

where e is the electron charge. From the results of Fig. 7, we get a transfer coefficient for the Tafel reaction of $\alpha \cong 0.65$.

The Heyrovsky reaction

We now turn to the Heyrovsky reaction:

$$H_{ad} + H^+ + e^- \rightarrow H_2$$

In this process, a proton from the double layer picks up an H^--like species on the surface to form an H_2 molecule without first adsorbing on the surface. The calculated minimum energy path is shown in Fig. 8. The initial coverage in this particular calculation is slightly above 1 (7/6 of a ML), and the H that is picked up is the on-top H atom. At a coverage below one, the reacting H adatom on the surface first has to move to the on-top position before this process can take place. The additional energy cost for doing this is small, ~0.1 eV. When there is an empty on-top site directly underneath the reacting proton, the NEB calculation gives a spontaneous discharge mechanism

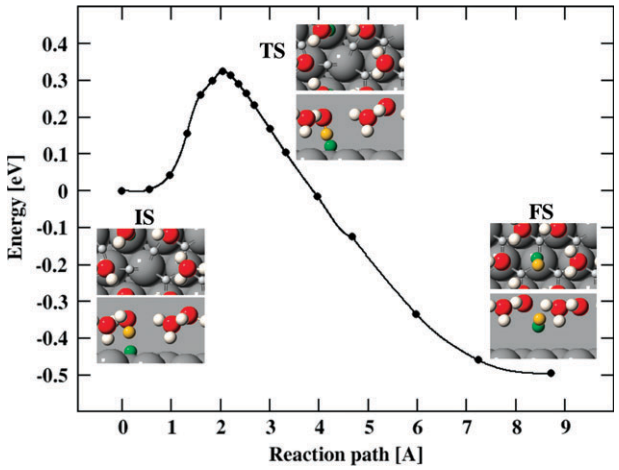

Fig. 8 Reaction path from NEB calculations showing the energy barrier for the Heyrovsky reaction ($H^+ + e^- + H_{ad} \rightarrow H_2$). The initial hydrogen coverage is 7/6 ML and a solvated proton reacts with on-top hydrogen, forming a H_2 molecule, which desorbs from the surface leaving 1 ML of hydrogen left on the surface. The average distance from the first Pt layer to the O atoms in the water bilayer is 3.76 Å for the IS and 4.60 Å for the FS.

corresponding to the Volmer reaction. We find a somewhat lower energy barrier for the Heyrovsky reaction than for the Tafel reaction in Fig. 5.

We now turn to the larger unit cell calculations where the potential can be varied by introducing additional protons/electrons. The results are summarized in Fig. 9. As expected, the variation in the reaction barrier with potential for the Heyrovsky reaction is substantial. We note that the value at the highly positive potential is hardly relevant to any experimental conditions since the reaction is very endothermic at these conditions; we include it only to show the variation of the activation energy with potential over a wide range. Comparison of Fig. 7 and Fig. 9 shows, however, that the activation energy for the Heyrovsky reaction is somewhat lower than for the Tafel reaction at a given potential.

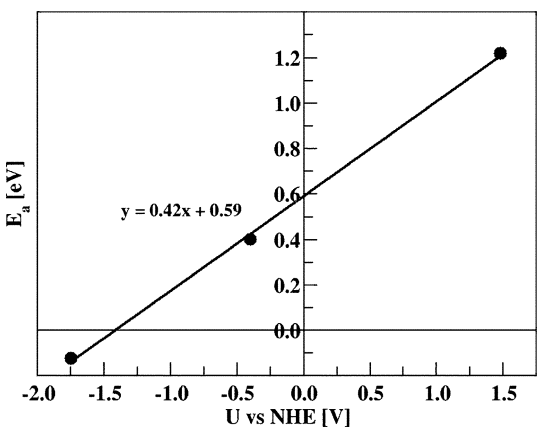

Fig. 9 Calculated activation energy *vs.* potential for the Heyrovsky reaction. The initial, transition and final states were calculated in three different super cells. For the most negative bias, the intermediate bias and the most positive bias, (6 × 2), (6 × 4) and (3 × 4) super cells were used with two, three and one hydronium ion(s) per unit cells and with initial hydrogen coverage of 22/12, 25/24 and 1/12 ML, respectively. The information in Fig. 4 has been used to determine the hydrogen coverage consistent with the potential generated by the hydronium ion concentration in the water bilayer. Here, we have included in the activation energy the energy cost of moving the adsorbed H atoms from an FCC site to an on-top site for the point at the most positive bias.

It should be noted that the method we use to obtain the electrode potential in these calculations is somewhat uncertain, particularly with respect to the absolute magnitude. The inclusion of more water layers could affect the calculated work function. Another uncertainty of the absolute potential is that ranges of values have been proposed for the shift, ϕ_{NHE}, used to determine U, see eqn (1). If we take the maximum value suggested for ϕ_{NHE} (4.85 V),[43] this would shift the whole curve in Fig. 9 left by 0.35 V, and the barrier for the Heyrovsky reaction at 0 V would increase by $\sim$0.15 eV, but it would still be smaller than that of the Tafel reaction at the same potential (note that the potential scale here is related to the coverage dependence only and thus comes from the adsorption free energies). The calculations, therefore, indicate that the Heyrovsky reaction is dominating. We are basing this conclusion on the calculated activation energy only. Entropic effects should also be taken into account, but given the magnitude of the difference in activation energy, it is likely that the conclusion would be the same even if the entropic barriers for the two reactions were somewhat different. Calculations of the vibrational frequencies for both the initial and transition states of the two reactions show all frequencies to be much larger than k_BT. In harmonic transition state theory this would suggest that the entropy factors are similar for the two mechanisms.

Similar to what was done for the Tafel reaction above, we can extract a transfer coefficient for the Heyrovsky reaction directly from the slope of the activation energy *vs.* potential (see Fig. 9). The value we find from the calculations is $\alpha \cong 0.4$. This is, again, in good agreement with measured values.[20] We note that this value is not affected by shifts in the estimates of the absolute value of the potential.

Discussion

If we combine the dependence of the coverage (Fig. 4) and activation energy (Fig. 9) on the potential we get the following overall picture: starting at positive values (relative to the normal hydrogen electrode) and lowering the potential U, hydrogen starts building up on the surface in FCC sites until it reaches a coverage of 1 around $U = 0$ V. Lowering the potential further does not lead to an increased coverage until approximately $U < -0.5$ V, at which point additional hydrogen is adsorbed in on-top sites. The present results therefore suggest that the H_{opd} adsorbed just below $U = 0$ V is a high coverage state with H adatoms mainly in FCC sites and only with a small fraction of thermally populated H in on-top sites, which is not very different from the low coverage H_{upd} state.

Below $U = 0$ V, hydrogen evolution becomes thermodynamically possible, and both the Tafel and the Heyrovsky reactions are found to have a moderate activation energy. The barrier for the Heyrovsky reaction is found to be lower and this suggests that the Heyrovsky reaction dominates, but

given the uncertainties in *e.g.* the determination of the overall electrode potential from the calculations, this conclusion is only tentative. We find that the Heyrovsky reaction proceeds by a proton from solution attacking a H atom in the on-top position. At all but the most negative potentials this means that the first step in the process is a transfer of a H atom from an FCC site to an on-top site on the surface. The energy difference between the two sites is very small ($\sim$0.1 eV).

Further insight into the origin of the transfer coefficient for the Heyrovsky reaction can be obtained from Fig. 10 where the calculated activation barrier is shown as a function of the reaction energy $\Delta E = E(\text{final}) - E(\text{initial})$. These calculations are all done with the large, (6 × 4) simulation cell and a coverage slightly above 1 ML (unlike Fig. 9 where the data points correspond to a coverage that is consistent with the electrode potential). The change in reaction energy originates in variations in the hydronium concentration in the simulated system. The correlation of the activation energy with the reaction energy is as good as with the potential, and the slope is essentially the same. We emphasize here that the reaction energy and the electrode potential extracted from the work function are independent variables, and that the variations in the activation barrier with electrode potential and H coverage are the same when plotted in this way. The result in Fig. 10 is analogous to the Brønsted–Evans–Polanyi relations between activation energy and reaction energy found throughout chemistry,[58] in particular in surface chemistry.[59–62] This relation has been assumed for a long time and the results of Fig. 10 represents a direct computational demonstration of the relation. The slope of approximately 0.45 indicates that the nature of the transition state is somewhere in-between that of the initial and the final state. This can also be seen in the insets in Fig. 8. The analogy between Fig. 9 and Fig. 10 confirms explicitly that the electrochemical transfer coefficient can be viewed as simply another manifestation of a Brønsted–Evans–Polanyi relation.

We note that the activation barrier (0.6 eV) obtained for the Heyrovsky reaction at $U = 0$ V is considerably larger than the one deduced from experiments (0.2 eV).[14] While there are definitely uncertainties relating to the methodology used in the calculations, the difference seems rather large. One possibility is that H atoms adsorbed on step sites are more reactive and could lead to a lower barrier. The magnitude of the calculated barrier, on the other hand, agrees quite well with the absolute values of the exchange current. As mentioned above, we find that the vibrational frequencies for both the initial and transition states of the Heyrovsky reaction are much larger than k_BT. According to harmonic transition state theory this suggests a prefactor, ν, of the order 10^{13} site^{-1} s^{-1} in an Arrhenius rate constant

$$k_0 = \nu \exp[-E_a/k_BT].$$

A typical value of the exchange current, i_0, on Pt(111) is 4.6×10^{-4} A cm^{-2},[21] and the surface area per Pt atom, A/N, is 6.64×10^{-16} cm^2. By applying

$$i_0 = k_0 eN/A$$

we get $k_0 \sim 0.95$ site^{-1} s^{-1}, which results in a E_a of 0.75 eV in quite good agreement with our calculations. Note that the 0.75 eV is the upper limit for E_a. Two effects could reduce the estimated barrier: a smaller prefactor and reduced number of reactive sites since only surface sites in contact with protons are active.

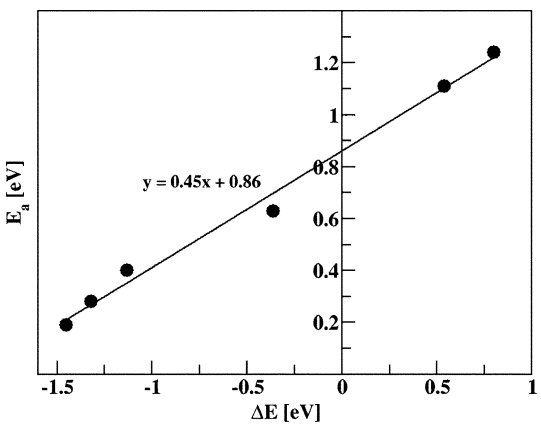

Fig. 10 Activation energy *vs.* reaction energy ($\Delta E = E_{\text{final}} - E_{\text{initial}}$) for the Heyrovsky reaction. A (6 × 4) super cell is used in all cases, with 1, 2, 3, or 4 protons and with initial hydrogen coverage of 25/24 or 28/24 ML.

In this connection it should be remembered that the method used here to estimate the effect of the electrode potential is approximate. The method could be made fully self-consistent if it were not for limitations in the system size and computational time available. The right hydrogen coverage would then be found by interpolation and used in simulations corresponding to a given value of the electrode potential. This self-consistency has only been achieved approximately in the present calculations. It is also important to realize that the potential affects the activation energy in different ways for the two reaction mechanisms. For the Tafel reaction, the variation in the activation energy occurs primarily through the variation of the hydrogen coverage, which is directly affected by the potential, but a change in the hydronium/electron concentration at a fixed coverage has little effect. For the Heyrovsky reaction, on the other hand, both the hydrogen coverage and the hydronium/electron concentration affect the activation barrier significantly.

For the Heyrovsky reaction we only consider the transfer of a proton from the double layer to the surface. There is an additional step where a proton from solution moves into the double layer to replace the proton that has reacted. We expect this step to have a barrier comparable to proton transfer in water, as for instance observed in connection with the Volmer reaction (*ca.* 0.15 eV, see Fig. 3). This is much lower than for the proton transfer to the surface, but the entropy barrier for this step could be much larger. This will require further study.

Conclusions

The present calculations provide a quite detailed picture of the electrochemical double layer during an electrochemical reaction. Our preliminary analysis of the results for the hydrogen evolution reaction gives a molecular level picture of the process, which is in good agreement with several experimental observations. We can understand the onset of H adsorption

and the subsequent onset of hydrogen evolution as the potential is decreased further. We find a strong potential dependence of the activation energy for both the Tafel and the Heyrovsky reactions, and the slope directly gives access to a theoretical value for the electrochemical transfer coefficient, ~ 0.65 for the Tafel reaction and ~ 0.4 for the Heyrovsky reaction. This is clearly in the range of values usually quoted for the HER.[19,20] The finding that the Heyrovsky reaction probably dominates is not in conflict with experimental observation, and the fact that the Tafel reaction is close in activation energy and can work in parallel, is in agreement with the observation that changing the surface structure is enough to change from one mechanism to another.[14]

The present calculations raise a number of questions. The most important discrepancy between theory and experiment from the present analysis is the large difference between the calculated and measured values of the activation energy. The procedure used for obtaining the electrode potential from the work function is another point where more work is needed. It would be desirable to develop a procedure where a closer self-consistency is reached between the hydrogen coverage on the electrode surface, hydronium concentration in the bilayer and the electrode potential, and where the electrode potential is more accurately estimated. We also need to include the transfer of protons from solution to the double layer. The present work also clearly points to the importance of being able to describe systems that are large enough so that the change in potential during a reaction is negligible. It would also be desirable to include more water in the simulation and to be able to distinguish between protons in solution and protons in the double layer.

Acknowledgements

We would like to thank Prof. Nenad Markovic, Prof. Eric M. Stuve and Dr Thomas Jaramillo for their valuable comments on the manuscript. The Center for Atomic-scale Materials Design is supported by the Lundbeck Foundation. This work was funded in part by the Danish Research Council for the Technical Sciences, the Danish NABIIT program, the Icelandic Research Foundation, and the Marie Curie research and training network 'Hydrogen'. The Danish Center for Scientific Computing contributed funding for the computer time.

References

1 N. M. Markovic and P. N. Ross, Jr, *Surf. Sci. Rep.*, 2002, **45**, 117.
2 K. Kunimatsu, T. Senzaki, M. Tsushima and M. Osawa, *Chem. Phys. Lett.*, 2005, **401**, 451.
3 S. Mukerjee, S. Srinivasan, M. P. Soriaga and J. McBreen, *J. Electrochem. Soc.*, 1995, **142**, 1409.
4 M. Teliska, V. S. Murthi, S. Mukerjee and D. E. Ramaker, *J. Electrochem. Soc.*, 2005, **152**, A2159.
5 R. J. K. Wiltshire, C. R. King, A. Rose, P. P. Wells, M. P. Hogarth, D. Thompsett and A. E. Russell, *Electrochim. Acta*, 2005, **50**, 5208.
6 E. M. Crabb, M. K. Ravikumar, Y. Qian, A. E. Russell, S. Maniguet, J. Yao, D. Thompsett, M. Hurford and S. C. Ball, *Electrochem. Solid-State Lett.*, 2002, **5**, A5.
7 G. Q. Lu, J. O. White and A. Wieckowski, *Surf. Sci.*, 2004, **564**, 131.
8 G. Q. Lu, A. Lagutchev, D. D. Dlott and A. Wieckowski, *Surf. Sci.*, 2005, **585**, 3.
9 A. Lagutchev, G. Q. Lu, T. Takeshita, D. D. Dlott and A. Wieckowski, *J. Chem. Phys.*, 2006, **125**, 154705.
10 D. L. Scovell, T. D. Pinkerton, V. K. Medvedev and E. M. Stuve, *Surf. Sci.*, 2000, **457**, 365.
11 T. Volmer and M. Erdey-Gruz, *Z. Phys. Chem., Abt. A*, 1930, **150**, 203.
12 J. Tafel, *Z. Phys. Chem., Stoechiom. Verwandtschaftsl.*, 1905, **50**, 641.
13 J. Heyrovsky, *Recl. Trav. Chim. Pays-Bas*, 1927, **46**, 582.
14 N. M. Markovic, B. N. Grgur and P. N. Ross, *J. Phys. Chem. B*, 1997, **101**, 5405.
15 B. E. Conway and G. Jerkiewicz, *Electrochim. Acta*, 2000, **45**, 4075.
16 J. Barber, S. Morin and B. E. Conway, *J. Electroanal. Chem.*, 1998, **446**, 125.
17 M. C. Tavares, S. A. S. Machado and L. H. Mazo, *Electrochim. Acta*, 2001, **46**, 4359.
18 J. X. Wang, T. E. Springer and R. R. Adzic, *J. Electrochem. Soc.*, 2006, **153**, A1732.
19 A. C. Fisher, *Electrode Dynamics*, Oxford University Press, Oxford, 2003, p. 6.
20 K. C. Neyerlin, W. Gu, J. Jorne and H. A. Gasteiger, *J. Electrochem. Soc.*, 2007, **154**, B631.
21 N. M. Markovic and P. N. Ross, in *Interfacial Electrochemistry—Theory, Experiments and Applications*, ed. A. Wieckowski, Marcel Dekker, New York, 1999.
22 B. E. Conway, J. Barber and S. Morin, *Electrochim. Acta*, 1998, **44**, 1109.
23 B. E. Conway, in *Interfacial Electrochemistry—Theory, Experiments and Applications*, ed. A. Wieckowski, Marcel Dekker, New York, 1999, p. 131.
24 Y. Cai and A. B. Anderson, *J. Phys. Chem. B*, 2004, **108**, 9829.
25 J. Greeley and M. Mavrikakis, *J. Am. Chem. Soc.*, 2004, **126**, 3910.
26 J. K. Nørskov, J. Rossmeisl, A. Logadottir, L. Lindqvist, J. R. Kitchin, T. Bligaard and H. Jónsson, *J. Phys. Chem. B*, 2004, **108**, 17886.
27 G. S. Karlberg, *Phys. Rev. B*, 2006, **74**, 153414.
28 J. S. Filhol and M. Neurock, *Angew. Chem., Int. Ed.*, 2006, **45**, 402.
29 T. E. Shubina and M. T. M. Koper, *Electrochem. Commun.*, 2006, **8**, 703.
30 P. Vassilev, R. A. van Santen and M. T. M. Koper, *J. Chem. Phys.*, 2005, **122**, 054701.
31 A. Roudgar and A. Gross, *Chem. Phys. Lett.*, 2005, **409**, 157.
32 Y. Okamoto, O. Sugino, Y. Mochizuki, T. Ikeshoji and Y. Morikawa, *Chem. Phys. Lett.*, 2003, **377**, 236.
33 J. K. Nørskov, T. Bligaard, A. Logadottir, J. R. Kitchin, J. G. Chen, S. Pandelov and U. Stimming, *J. Electrochem. Soc.*, 2005, **152**, J23.
34 M. Otani and O. Sugino, *Phys. Rev. B*, 2006, **73**, 115407.
35 M. C. Payne, M. P. Teter, D. C. Allan, T. A. Arias and J. D. Joannopoulos, *Rev. Mod. Phys.*, 1992, **64**, 1045.
36 G. Kresse and J. Furtmüller, *Comput. Mater. Sci.*, 1996, **6**, 15.
37 D. Vanderbilt, *Phys. Rev. B*, 1990, **41**, 7892.
38 B. Hammer, L. B. Hansen and J. K. Nørskov, *Phys. Rev. B*, 1999, **59**, 7413.
39 Dacapo pseudopotential code, URL: https://wiki.fysik.dtu.dk/dacapo, Center for Atomic-scale Materials Design (CAMD), Technical University of Denmark, Lyngby, 2006.
40 M. A. Henderson, *Surf. Sci. Rep.*, 2002, **46**, 216–217, and references therein.
41 S. Trasatti, *Electrochim. Acta*, 1991, **36**, 1657.
42 J. E. B. Randles, *Trans. Faraday Soc.*, 1956, **52**, 1573.
43 E. R. Kötz, H. Neff and K. Müller, *J. Electroanal. Chem.*, 1986, **215**, 331.
44 H. Jónsson, G. Mills and K. W. Jacobsen, in *Classical and Quantum Dynamics in Condensed Phase Simulations*, ed. B. J. Berne, G. Ciccotti and D. F. Coker, World Scientific, Singapore, 1998.
45 G. Henkelman and H. Jónsson, *J. Chem. Phys.*, 2000, **113**, 9978.
46 N. Agmon, *Chem. Phys. Lett.*, 1995, **244**, 456.
47 J. P. Guthrie, *J. Am. Chem. Soc.*, 1996, **118**, 12886.
48 O. Pecina and W. Schmickler, *Chem. Phys.*, 1998, **128**, 265.
49 J. Rossmeisl, J. K. Nørskov, C. D. Taylor, M. J. Janik and M. Neurock, *J. Phys. Chem. B*, 2006, **110**, 21833.
50 G. Jerkiewicz, *Prog. Surf. Sci.*, 1998, **47**, 137.
51 R. J. Nichols and A. Bewick, *J. Electroanal. Chem.*, 1988, **243**, 445.

52 A. M. Baro, H. Ibach and H. D. Brushman, *Surf. Sci.*, 1979, **88**, 384.
53 L. J. Richter and W. Ho, *Phys. Rev. B*, 1987, **36**, 9797.
54 J. E. Reutt, Y. J. Chabal and S. B. Christman, *J. Electron Spectrosc. Relat. Phenom.*, 1987, **44**, 325.
55 G. Källén and G. Wahnström, *Phys. Rev. B*, 2001, **65**, 033406.
56 K. Christmann, G. Ertl and T. Piget, *Surf. Sci. Rep.*, 1976, **54**, 365.
57 B. Poelsema, R. L. Palmer, G. Mechtersheimer and G. Comsa, *Surf. Sci.*, 1980, **117**, 60.
58 L. P. Hammett and M. A. Paul, *J. Am. Chem. Soc.*, 1934, **56**, 830.
59 J. K. Nørskov, T. Bligaard, A. Logadottir, S. Bahn, M. Bollinger, L. B. Hansen, H. Bengaard, B. Hammer, Z. Sljivancanin, M. Mavrikakis, Y. Xu, S. Dahl and C. J. H. Jacobsen, *J. Catal.*, 2002, **209**, 275.
60 V. Pallasana and M. Neurock, *J. Catal.*, 2000, **191**, 301.
61 Z. P. Liu and P. Hu, *J. Chem. Phys.*, 2001, **114**, 8244.
62 A. Logadottir, T. H. Rod, J. K. Nørskov, B. Hammer, S. Dahl and C. J. H. Jacobsen, *J. Catal.*, 2001, **197**, 229.

